



Excess radiation exacerbates drought stress impacts on stomatal conductance along aridity gradients

Jing Wang¹, Xuefa Wen^{1,2,3}

¹Key Laboratory of Ecosystem Network Observation and Modeling, Institute of Geographic Sciences and Natural Resources Research, Chinese Academy of Sciences, Beijing, 100101, China

²College of Resources and Environment, University of Chinese Academy of Sciences, Beijing, 101408, China

³Beijing Yanshan Earth Critical Zone National Research Station, University of Chinese Academy of Sciences, Beijing, 101408, China

Correspondence to: Xuefa Wen (wenxf@igsnr.ac.cn) and Jing Wang (wangjing.15b@igsnr.ac.cn)

Abstract. Stomatal conductance (g_s) of all co-existing species regulates transpiration in arid and semi-arid grasslands prone to droughts. However, the effect of drought stress on g_s is debated, and the interaction effects of abiotic and biotic constraints on canopy g_s remain poorly understood. Here, we used ^{18}O enrichment of leaf organic matter above source water ($\Delta^{18}\text{O}$) as proxy for g_s per leaf area to increase understanding of these effects. Three grassland transects were established along aridity gradients in Loess Plateau (LP), Inner Mongolian Plateau (MP), and Tibetan Plateau (TP) which differ in radiation and temperature conditions. Results showed that canopy g_s consistently decreased with increasing aridity within transects. The order of g_s at a given aridity index was LP>MP>TP, due to suppressed effects of excess radiation and low temperatures among transects. Primary determinant of drought stress on g_s was soil moisture (SM) in LP and MP, and vapor pressure deficit (VPD) in TP. Radiation exhibited consistently negative effect on g_s via drought stress within transects, while temperature had positive effects on g_s in LP, no effects in MP, and negative effects in TP. Adding the interaction of leaf area and abiotic factors increases the percent of explained variability in g_s by 17 and 36% in LP and MP, respectively, but not in TP due to an overwhelming effect of climate. The results highlighted the need to integrate multiple stressors and plant properties to determine spatial variability in g_s .

Keywords: stomatal conductance, oxygen isotope, drought stress, excess radiation, high temperature, grassland

1 Introduction

Stomatal conductance (g_s) of all co-existing species plays a significant role in water loss (transpiration) and carbon uptake (photosynthesis) at ecosystem level, thereby coupling water and carbon cycles (Jarvis & McNaughton, 1986; Zhu *et al.*, 2015; Martin-StPaul *et al.*, 2017; Wang *et al.*, 2021a). The model linkages between g_s and photosynthesis mean that the biophysical response of g_s varies depending on water, radiation, temperature and leaf economic traits at leaf level (Farquhar *et al.*, 1980; Leuning, 1995; Wright *et al.*, 2004; Buckley, 2019; Carminati & Javaux, 2020). However, experimental evidence suggested that the strength of g_s responses to changing environment factors varies with species (Galmes *et al.*, 2007), and changes in



environment factors can have interactive effects on the variability in g_s (Zeuthen *et al.*, 1997; Costa *et al.*, 2015; Doupis *et al.*, 2020). Community in field is simultaneously affected by a variety of environmental stressors, and canopy g_s is the cumulative rate over time of co-occurring species (Xia *et al.*, 2015). However, how interactive effects of multiple environment stressors and community traits regulate the spatial patterns of canopy g_s remain largely unknown (Maxwell *et al.*, 2018).

35 Drylands cover 41% of the Earth's surface (Yao *et al.*, 2020; Xu *et al.*, 2021b), and drive the variability in global terrestrial carbon sink (Ahlstrom *et al.*, 2015). The survival, transpiration, and productivity of plants growing in this region is simultaneously stressed by drought (Hoshika *et al.*, 2018; Peters *et al.*, 2018; Flo *et al.*, 2021), high solar radiation and temperature (Peguero-Pina *et al.*, 2020). In addition, communities respond to drought, solar radiation and temperature stressors by changing their functional traits (Fyllas *et al.*, 2017; Martin-StPaul *et al.*, 2017; Aguirre-Gutierrez *et al.*, 2019); this may
40 ultimately affect g_s (Wang *et al.*, 2021b). Thus, canopy g_s in drylands was expected to be influenced by the interaction of drought, high radiation, high temperature and biotic factors.

Canopy g_s should be primarily limited by drought in drylands, which is often characterized as low soil moisture (SM) and high vapor pressure deficit (VPD). It is generally assumed that increased drought stress reduces g_s at leaf level (Hoshika *et al.*, 2018; Peters *et al.*, 2018; Stocker *et al.*, 2019; Flo *et al.*, 2021). The limitation of SM and VPD on g_s involves two
45 independent mechanisms; in one, low SM (available water in the soil for plant root uptake) reduces soil water potential and hinders transport of soil water to leaf; in the other, high VPD reduces leaf water potential and increases transpiration demand (Oren *et al.*, 1999; Buckley, 2017; Zhang *et al.*, 2021). However, there is an ongoing debate on the relative role of SM and VPD in determining the response of canopy g_s to dryness (Liu *et al.*, 2020). For instance, a global analysis demonstrated that SM stress is the dominant driver of productivity in semi-arid ecosystems (Liu *et al.*, 2020). However, another study
50 demonstrated that VPD stress is the dominant influence on surface conductance (Konings *et al.*, 2017). Yet, these studies lack direct biological evidence, because canopy g_s cannot be measured directly, especially at large scales.

Radiation and temperature may indirectly regulate canopy g_s by influencing photosynthesis (Aasamaa & Sober, 2011; Medlyn *et al.*, 2012) and adjusting drought stress (Ciais *et al.*, 2005). However, previous studies conducted at leaf level showed that the direction and intensity of radiation and temperature on g_s strongly depend on their distribution range and the
55 relationship with aridity. For example, the response of g_s to radiation and temperature generally shows an increasing trend up to optimum values (Xu *et al.*, 2021a), while excess radiation in combination with drought stress suppresses g_s (Zeuthen *et al.*, 1997; Costa *et al.*, 2015; Doupis *et al.*, 2020). In addition, increasing temperature may result in high VPD or low SM (Seneviratne *et al.*, 2010). However, these effects were obscured by drought stress in natural conditions, which alone caused a g_s reduction (Fu *et al.*, 2006; Duan *et al.*, 2008). Consequently, it is difficult to disentangle whether the decline in g_s at
60 community level with increasing aridity is simply a consequence of drought stress or an interaction of multiple stressors.

Additionally, environmental stressors should have an indirect effect on canopy g_s by regulating community morphological traits. However, few studies have addressed this topic at the community scale considering both environmental



and plant regulators. Communities change their morphological functional traits to tolerate environmental stress (Anderegg *et al.*, 2018), including leaf area (LA) and specific leaf area (SLA) (Wright *et al.*, 2017). LA and SLA determine plant capacity
65 for capturing light (Poorter *et al.*, 2009), leaf heat exchange (Wright *et al.*, 2017), and length of water pathway through leaves
(Kang *et al.*, 2021), all of which are closely related to transpiration and photosynthesis. Previous studies focused primarily on
the patterns of LA and SLA along environmental gradients (Peppe *et al.*, 2011; Wright *et al.*, 2017). For example, small-leaved
species prevail in dry, hot, sunny environments, or at high elevations (Wright *et al.*, 2017). SLA generally decreases with
increasing radiation and drought stress, and increases with decreases in temperature (Poorter *et al.*, 2009). Recently, a study
70 conducted in woody species in eastern Qinghai-Tibet, China showed that LA and stomatal size co-varied with temperature
(Kang *et al.*, 2021), indicating that the changes in LA and SLA may play important roles in regulating canopy gs.

To investigate the interactive effect of environmental stressors and biotic factors on canopy gs, three grassland transects
along aridity gradients were established in three plateaus with different radiation and temperature conditions, i.e., Loess Plateau
(LP), Mongolian Plateau (MP), and Tibetan Plateau (TP) across arid and semi-arid regions in China. Given that the order of
75 mean annual temperature and radiation is LP>MP>TP and LP<MP<TP, respectively (Ren *et al.*, 2021), the differences in
radiation and temperature across three plateaus provide an ideal platform for exploration of interaction effects of multiple
stressors and biotic factors on canopy gs. We hypothesized that: (1) increasing solar radiation and/or air temperature along
aridity gradient will exacerbate drought stress impacts on gs within transects, (2) excess solar radiation and low temperatures
will result in differences in gs among transects, (3) integrating environmental stress and community functional traits will
80 significantly improve the capacity for predicting gs.

Bulk leaf $\delta^{18}\text{O}$ and aboveground biomass of all co-existing species were determined. Theoretically, the change of $\delta^{18}\text{O}$ in
organic matter is affected by gs based in steady-state leaf water ^{18}O enrichment (Farquhar *et al.*, 1998; Barbour *et al.*, 2000;
Barbour, 2007). Negative relationship between $\delta^{18}\text{O}$ (or the ^{18}O enrichment of organic matter above source water, $\Delta^{18}\text{O}$) and
gs expected relationship has been observed intra- (Cernusak *et al.*, 2009; Cabrera-Bosquet *et al.*, 2011) and inter-species
85 (Barbour *et al.*, 2000; Grams *et al.*, 2007; Cernusak *et al.*, 2009; Moreno-Gutierrez *et al.*, 2012), and among communities
along a climate gradient (Keitel *et al.*, 2006). $\delta^{18}\text{O}$ or $\Delta^{18}\text{O}$ is now widely used by plant eco-physiologists to infer the spatial
and temporal variation in gs (Flanagan & Farquhar, 2014; Maxwell *et al.*, 2018; Guerrieri *et al.*, 2019; Levesque *et al.*, 2019).
To exclude the influence of variation in $\delta^{18}\text{O}$ of the source water, we calculated the $\Delta^{18}\text{O}$ (Keitel *et al.*, 2006). Combining
with aboveground biomass, $1/\Delta^{18}\text{O}$ was upscaled from leaf to community levels (Flanagan & Farquhar, 2014; Wang *et al.*,
90 2021b). Proxies for drought (i.e., SM and VPD), air temperature (i.e., mean, maximum and minimum) and solar radiation were
derived from global or regional datasets.



2 Materials and methods

2.1 Study areas

In this study, we established three grassland transects spanning a broad range of climatic conditions and grassland types in arid and semi-arid regions (i.e., Loess Plateau, LP; Inner Mongolian Plateau, MP; Tibetan Plateau, TP) in China (Lyu *et al.*, 2021). Transects were 600 km long in LP, 1200 km in MP, and 1500 km in TP. Differences in aridity (calculated as $1 - \text{mean annual precipitation/potential evapotranspiration}$) and growing season precipitation were not significant ($P > 0.05$) among transects, while there are significant differences in growth season air temperature ($LP > MP > TP$) (Fig. 1c) and solar radiation ($LP < MP < TP$) (Fig. 1d) among transects. In each transect, we selected 10 sampling sites with increasing aridity index (Fig. 1e) and growing season solar radiation (Fig. 1h), and decreasing growing season precipitation from east to west (Fig. 1f). More details about the characteristics of climate, soil and vegetation type in the 30 sampling sites can be found in (Lyu *et al.*, 2021).

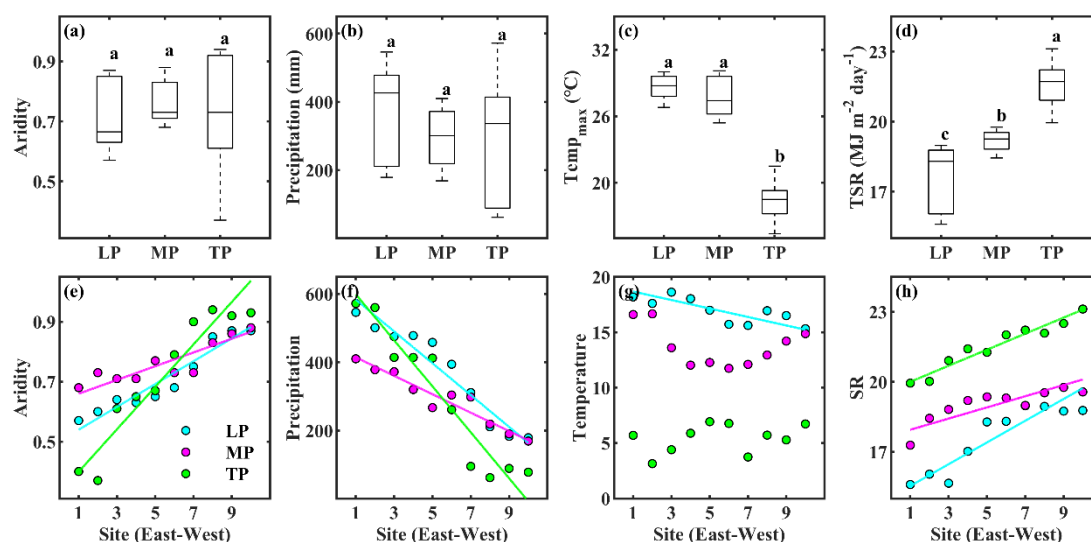


Figure 1. Comparison of aridity, growing season precipitation (mm), air temperature ($^{\circ}\text{C}$), and radiation ($\text{MJ m}^{-2} \text{day}^{-1}$) (a) among three transects and (b) within transects. LP: Loess Plateau; MP, Inner Mongolia Plateau; TP, Tibet Plateau. Lowercase letters indicate significant differences among transects ($P < 0.05$). Error bars indicate standard error of the mean.

2.2 Sampling and measurements

2.2.1 Sample processing

A field survey and sample collection were conducted during the peak growing season (July to August) in 2018. Within each of 30 sites, we delineated eight $1\text{m} \times 1\text{m}$ plots in a $100\text{m} \times 100\text{m}$ sampling area (Lyu *et al.*, 2021). Plant species (identified by experienced plant taxonomists), number of species and community structure were surveyed. Aboveground biomass was collected by species for dry mass and stable isotope analyses.



2.2.2 Leaf area and SLA analysis

Three individuals were collected as replications for each species, six to ten fresh, healthy, and mature leaves were selected from individuals of each species, and leaf area (LA) was determined using a portable scanner (Cano Scan LIDE 110, Japan).
115 Image J software was used to obtain LA values (Schneider *et al.*, 2012). Then, leaves were dried at 60°C and weighed for leaf dry mass. SLA was calculated by dividing LA by leaf dry mass.

2.2.3 Stable isotope analysis

In this study, we used $1/\Delta^{18}\text{O}$ in bulk leaves as proxy for $\text{gs. } \Delta^{18}\text{O}$ at species level ($\Delta^{18}\text{O}_L$) was calculated as (Wang *et al.*, 2021b):

$$120 \quad \Delta^{18}\text{O}_L = \frac{(\delta^{18}\text{O}_L - \delta^{18}\text{O}_P)}{(1 + \delta^{18}\text{O}_P/1000)} \quad (1)$$

where $\delta^{18}\text{O}_L$ is bulk-leaf $\delta^{18}\text{O}$ at species level; $\delta^{18}\text{O}_P$ is the amount-weighted $\delta^{18}\text{O}$ of precipitation during the growing season. $\delta^{18}\text{O}$ of monthly precipitation at each site was simulated using longitude, latitude, and elevation according to (Bowen *et al.*, 2005).

We measured $\delta^{18}\text{O}$ values in bulk leaves. Dried leaf samples were ground using a ball mill, and oven dried before analysis.
125 Leaf samples were prepared in silver capsules for $\delta^{18}\text{O}$ analysis. An isotope ratio mass spectrometer in continuous-flow mode (Model 253 plus, Thermo Fisher Scientific, Bremen, Germany) coupled with an elemental analyzer (Model Flash 2000HT, Thermo Fisher Scientific, Bremen, Germany) was used to determine $\delta^{18}\text{O}$ values. Isotope ratios are expressed as per mil deviations relative to VSMOW (oxygen) standards. Long-term precision for the instrument was $< 0.2\%$ for $\delta^{18}\text{O}$ measurements.

2.3 Community $1/\Delta^{18}\text{O}$, LA and SLA

130 Plant community parameters ($1/\Delta^{18}\text{O}$, LA and SLA) were defined for each sampling site, and calculated as an average of eight quadrats. The $1/\Delta^{18}\text{O}$, LA, and SLA were scaled from leaf to community levels as follows (Wang *et al.*, 2021b):

$$1/\Delta^{18}\text{O} = \sum_n^i \text{BF}_i \times (1/\Delta^{18}\text{O}_L)_i \quad (2)$$

$$\text{LA} = \sum_n^i \text{BF}_i \times (\text{LA}_L)_i \quad (3)$$



$$SLA = \sum_n^i BF_i \times (SLA_L)_i \quad (4)$$

135 where n is the species richness (number of species) of the community, and BF_i is the ratio of aboveground biomass of the i th species to the total aboveground biomass of the community. LA_L and SLA_L represent values of LA and SLA at leaf scale. Aboveground biomass of each species was obtained by directly weighing dried plant tissue per quadrat.

2.4 Auxiliary dataset

Climate variables were obtained from the standard (19) WorldClim Bioclimatic variables for WorldClim version 2 (1 km²)
140 (<https://www.worldclim.org/>) (Fick & Hijmans 2017). The growing season (April to October) and annual mean air temperature, maximum temperature, minimum temperature, actual water vapor pressure, and cumulative precipitation were calculated from monthly values. Vapor pressure deficit (VPD) was calculated from actual water vapor pressure and temperature (Grossiord *et al.*, 2020). Aridity index (=1-MAP/potential evapotranspiration) was extracted from the CGIAR-CSI
145 (<https://cgiarcsi.community>). Solar radiation was derived from “A dataset of reconstructed photosynthetically active radiation in China (1961 – 2014)” (Liu *et al.*, 2017). Soil moisture content within the top 10 cm depth was extracted from remote-sensing-based surface soil moisture (RSSSM) dataset at 0.1° spatial resolution (Chen *et al.*, 2021), and approximately 10-day temporal resolution.

2.5 Statistical analysis

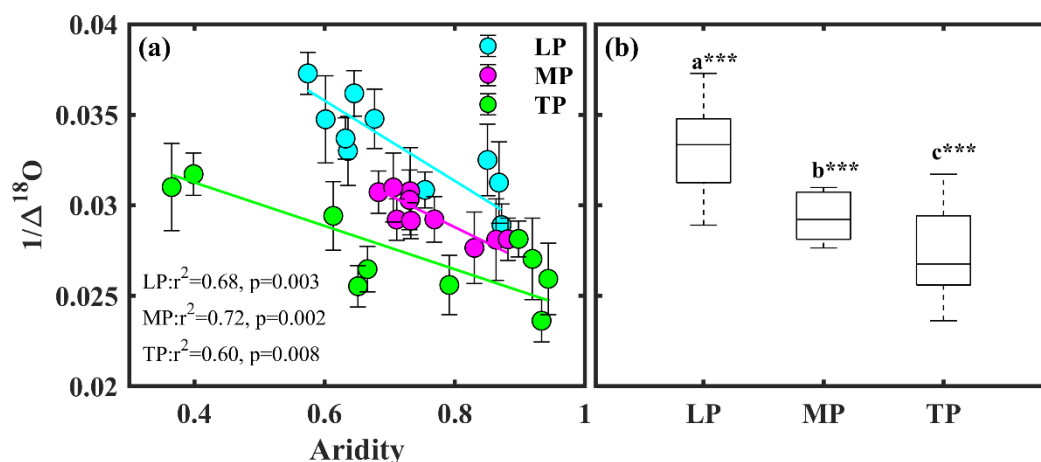
Differences in climate variables among three transects were tested with a one-way ANOVA with Duncan’s post hoc multiple
150 comparisons (SPSS, Chicago, IL, USA). To explore bivariate relationships between each of our hypothesized drivers (water variables and plant attributes) and g_s , we conducted Pearson correlation analyses using IBM SPSS 20 software (SPSS, Chicago, IL). Linear regressions were used to describe the relationships between g_s and aridity (Matlab, Version 2018b). We further tested the differences in slopes and intercepts of linear regression between g_s and aridity using standardized major axis (SMA) regression fits (Wright *et al.*, 2006) (R Core Team 2012). To determine the interactive effects of climate variables and plant
155 properties on variability in g_s along an aridity gradient, we fitted structural equation models using the “lavaan” package in R statistical program (R Core Team 2012) based on the current knowledge of the interactive relationships between climate variables, plant properties, and g_s . We chose the final models with high-fit statistics: comparative fit index >0.95, standardized root mean square residual < 0.08, and p-value > 0.8.



3 Results

160 3.1 Variability in $1/\Delta^{18}\text{O}$ along aridity gradients

Bivariate linear regression of $1/\Delta^{18}\text{O}$ on aridity showed that $1/\Delta^{18}\text{O}$ decreased linearly with increasing aridity within transects (Fig.2a). The standardized major axis (SMA) regression fits demonstrated that intercepts of SMA were significantly different from each other ($P < 0.05$), while the slopes were not ($P > 0.05$). The order of the intercepts was Loess Plateau (LP) < Inner Mongolia (MP) < Tibet Plateau (TP) ($P < 0.05$, Table S1). The intercepts of SMA did not exhibited relationship with precipitation (Fig.3a, $P > 0.05$), decreased with decreasing temperature (Fig.3b, $P < 0.01$), and increased with increasing solar radiation (Fig.3c, $P < 0.05$). Significant differences in gs were found among transects ($P < 0.001$), and the order was LP > MP > TP (Fig.2b).



170 **Figure 2.** Patterns of $1/\Delta^{18}\text{O}$ (a) along aridity gradient within transects, and among (b) transects. Different letters indicate significant differences ($P < 0.001$) among transects and grassland types. LP, Loess Plateau; MP, Inner Mongolia Plateau; TP, Tibet Plateau.

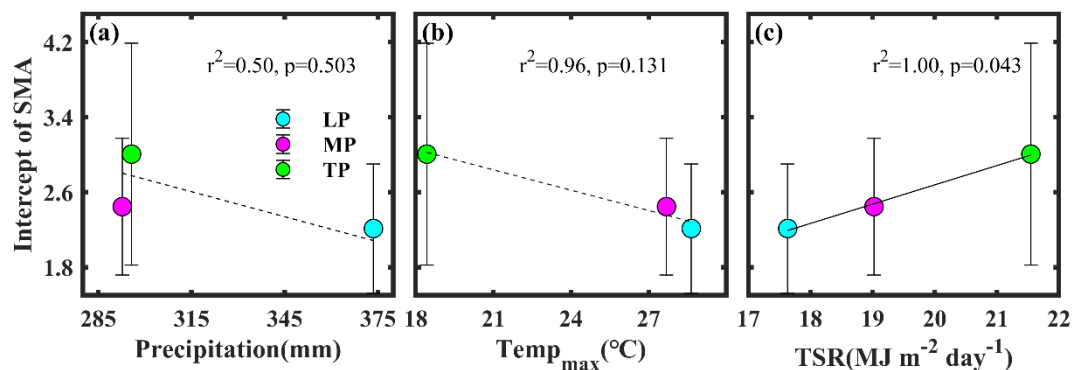


Figure 3. The relationship between the intercept obtained from standardized major axis analysis (SMA) and growing season (a) precipitation, (b) temperature, and (c) solar radiation (SR).



3.2 Effects of SM and VPD on the variability in $1/\Delta^{18}\text{O}$

175 Pearson correlation analysis showed that $1/\Delta^{18}\text{O}$ was positively correlated with soil moisture (SM) along aridity gradients within three transects ($P < 0.05$, Table 1), while a significant relationship between $1/\Delta^{18}\text{O}$ and vapor pressure deficit (VPD) was observed only in TP ($P < 0.01$). Solar radiation (SR) exhibited negative correlations with $1/\Delta^{18}\text{O}$ in all three Plateaus ($P < 0.05$). Both mean ($\text{Temp}_{\text{mean}}$) and maximum (Temp_{max}) temperatures were significantly and positively correlated with $1/\Delta^{18}\text{O}$ in LP, but negatively in TP. However, there were no significant correlations between both $\text{Temp}_{\text{mean}}$ and Temp_{max} and $1/\Delta^{18}\text{O}$ in MP. Positive correlations were found between g_s and leaf area (LA) in LP and MP, and negative between $1/\Delta^{18}\text{O}$ and specific leaf area (SLA) in TP ($P < 0.05$).

Table 1 Pearson's coefficients among stomatal conductance (g_s , using $1/\Delta^{18}\text{O}$ as proxy for g_s) and environmental factors and plant properties.

| | Loess Plateau | Inner Mongolia Plateau | Tibet Plateau |
|-----------------------------|---------------|------------------------|---------------|
| Aridity | -0.848** | -0.843** | -0.773** |
| SM | 0.719* | 0.707* | 0.659* |
| VPD | -0.554 | -0.384 | -0.912** |
| SR | -0.639* | -0.728* | -0.850** |
| $\text{Temp}_{\text{mean}}$ | 0.641* | 0.303 | -0.670* |
| Temp_{max} | 0.678* | 0.038 | -0.852** |
| LA | 0.757* | 0.913** | 0.610 |
| SLA | -0.519 | -0.576 | -0.648* |

185 **, $P < 0.01$; *, $P < 0.05$. SM, soil moisture; VPD, vapor pressure deficit; SR, total solar radiation; $\text{Temp}_{\text{mean}}$, mean temperature; Temp_{max} , maximum temperature; LA, leaf area; SLA, specific leaf area.

The interaction effects of environmental factors (Table 1) on $1/\Delta^{18}\text{O}$ within transects were determined with structural equation models (SEMs) (Fig.4a-c). SR, acting via SM, exhibited the strongest influence on $1/\Delta^{18}\text{O}$ in LP (standardized path coefficient of indirect effect [SPCI]= -0.52) (Fig.4a). Temp_{max} in LP showed a weak and positive indirect effect on $1/\Delta^{18}\text{O}$ via SM (SPCI = 0.14). SR in MP exhibited a negative indirect effect on g_s via SM (SPCI = -0.53) (Fig.4b). The negative indirect effects of SR (SPCI = -0.49) and Temp_{max} (SPCI = -0.45) on g_s via VPD in TP were similar (Fig.4c). The effect of



SR on $Temp_{max}$ was inconsistent among transects: SR had a negative effect on $Temp_{max}$ in LP, a positive effect in TP, and no effect in MP.

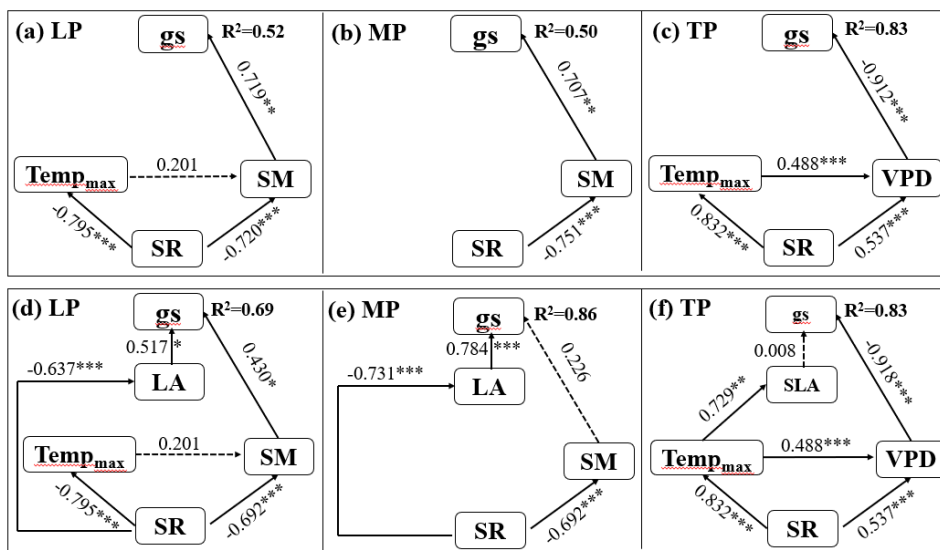


Figure 4. Structural equation models for stomatal conductance (gs). gs, stomatal conductance (using $1/\Delta^{18}O$ as proxy for gs); $Temp_{max}$: maximum temperature; SR, solar radiation; SM, soil moisture; VPD, vapor pressure deficit; LA, leaf area; SLA, specific leaf area; LP, Loess Plateau; MP, Inner Mongolia Plateau; TP, Tibet Plateau.

3.3 Interaction effects of abiotic and biotic factors on the variability in $1/\Delta^{18}O$

When leaf area and specific leaf area were incorporated into the SEM, $1/\Delta^{18}O$ prediction significantly improved in LP and MP (Fig.4d-f), but there was no change in TP. In particular, LA had a positive effect on $1/\Delta^{18}O$ in LP, and its effect [SPC=0.517] was slightly larger than that of SM [SPC=0.430] (Fig.4d). LA exhibited a positive direct effect on $1/\Delta^{18}O$ in MP (Fig. 4d), while the effect of SM was not statistically significant (Fig.4e). However, SLA did not directly affect $1/\Delta^{18}O$ in TP ($P>0.05$) (Fig.4f).

4 Discussion

4.1 Different patterns of gs across transects

Stomatal conductance (gs, using $1/\Delta^{18}O$ as proxy for gs) consistently decreased with increasing aridity within the three transects; the order of gs at a given aridity value was Loess Plateau (LP) > Inner Mongolia Plateau (MP) > Tibetan Plateau (TP) (Fig.2a, Table S1). We attributed the differences among transects to the suppressed effects of excess radiation and low temperature due to the significant decrease in average growing season temperature (Fig.3b) and increase in solar radiation



(Fig.3c) from LP to TP. Given that g_s is typically correlated with photosynthesis (Aasamaa & Sober, 2011; Medlyn *et al.*, 2012), radiation and temperature may indirectly regulate g_s by influencing photosynthesis (Aasamaa & Sober, 2011; Medlyn *et al.*, 2012). Photosynthesis generally increased with increasing radiation and temperature until optimum values (Mercado *et al.*, 2009; Wehr *et al.*, 2017). Consequently, photosynthesis was lower in a cold than in a warm environment (Zhang *et al.*, 2018). In addition, excess radiation would suppress photosynthesis via photoinhibition (Demmig-Adams & Adams, 1992).

The relationship between intercepts of standardized major axis (SMA) and maximum temperature and solar radiation (Fig.3) further supports our view that excess radiation and low temperature interacted to exacerbate drought stress impacts on g_s among transects. The intercepts of SMA significantly increased with decreasing temperature ($P < 0.01$, Fig.3b) and increasing solar radiation ($P < 0.01$, Fig.3c). Consequently, g_s in TP was smaller than in LP and MP at given aridity conditions because the environment in TP is characterized by low temperature and high radiation.

4.2 Radiation and temperature regulates variability in g_s via drought stress within transects

Based on results from this and earlier studies, we conclude that the decreasing g_s with increasing aridity within transects was mainly due to drought stress, coupled with effects of high solar radiation or/and temperature. The relative roles of soil moisture (SM) and vapor pressure deficit (VPD) in restricting g_s along an aridity gradient were different across the three transects (Table 1). Fu *et al.* (2006) found that the primary g_s -limiting factor was drought stress. In this study, we found that the variability in g_s was limited by SM in LP and MP, and co-limited by SM and VPD in TP. In addition, a global meta-analysis demonstrated that ecosystem productivity was limited by low SM regardless of VPD when drought stress was dominated by SM, and vice versa (Liu *et al.*, 2020). It meant that drought stress may be primarily controlled by SM in LP and MP, but may be limited by both SM and VPD in TP. An eddy covariance study conducted at an observation site in TP demonstrated that gross primary productivity (GPP) in the growing season was significantly limited by SM and VPD, however, the accumulated GPP was primarily determined by SM (Xu *et al.*, 2021b). This may be because the dominant factors of drought stress differ for different spatial and temporal scales.

Solar radiation and temperature regulated variability in g_s within transect via drought stress (Fig.4). Solar radiation exhibited consistently negative effects on g_s , because it increased with increasing aridity within three transects (Fig.1h, Table S2). These results were consistent with those of Fu *et al.* (2006), who demonstrated that the net CO_2 exchange of grassland in MP and shrubland in TP was significantly reduced by high solar radiation.

On one hand, increasing radiation decreased SM by regulating evaporation and transpiration (Zhang *et al.*, 2019). Solar radiation had negative effects on SM in the three transects in this study (Table S2). Meanwhile, increasing solar radiation can increase VPD by increasing temperatures (Grossiord *et al.*, 2020). However, a positive relationship between temperature and VPD was observed only in TP (Table S2).



On the other hand, excess ultraviolet-B radiation (Duan *et al.*, 2008), insufficient thermal dissipation, and enhanced
240 photorespiration under high solar radiation (Cui *et al.*, 2003) can decrease photosynthesis, ultimately reducing g_s . For example,
photosynthesis in two herbaceous species in TP was reduced due to photorespiration in conditions of high photosynthetic
photon flux density (Cui *et al.*, 2003).

The effect of temperature on variability in g_s within transects differed among transects: drought stress effects on g_s can
be partly mitigated by lower temperatures in LP (Fig.4a), but exacerbated by higher temperatures in TP (Fig.4c). As with
245 radiation, increases in temperature tend to increase evaporation and transpiration rates ultimately reducing SM, while VPD
can be expressed as a curvilinear function of air temperature (Lawrence, 2005), always increasing with increasing temperatures
(Oren *et al.*, 1999; Grossiord *et al.*, 2020).

g_s exhibits a bell-shape response to air temperature (Li *et al.*, 2020). A leaf-level study conducted in TP showed that g_s
increased with increasing air temperatures until a maximum at 24.8 °C, and then declined (Li *et al.*, 2020). Ecosystem-level
250 studies also showed that high temperature at noon can result in a partial stomatal closure, ultimately limiting g_s (Fu *et al.*, 2006;
Zhang *et al.*, 2018). In TP, maximum temperature increased with increasing aridity, and was negatively related to SM and
positively to VPD (Table S2, Fig.4c). Consequently, maximum temperature may exacerbate soil and atmospheric drought, and
inhibit transpiration and photosynthesis, ultimately reducing g_s along an aridity gradient. However, the maximum temperature
decreased with increasing aridity in LP, and exhibited a positive effect on SM (Table S2). Under this hydrothermal
255 synchronization effect, the maximum temperature exhibits a positive effect on g_s .

4.3 Interacting effects of abiotic and biotic factors on the variability in g_s within transects

Our findings indicated that radiation and temperature indirectly regulated variability in g_s along an aridity gradient within
transects through leaf morphological properties. Including leaf area (LA) increased the percentage of explained variability in
 g_s by 17 and 36% in LP and MP, respectively (Fig.4d-e), compared to SEM models which excluded plant variables. This
260 highlighted the need to integrate plant properties related to light capture and heat exchange when examining spatial variability
in g_s . To the best of our knowledge, this study was the first in which leaf morphological properties were included to quantify
the relative contributions of climate and plant on g_s . Specifically, solar radiation exhibited negative effects on g_s via LA in LP
and MP (Fig.4d-e). Kang *et al.* (2021) noted that plants tend to balance light capture with damage from high solar radiation.
Solar radiation increased with increasing aridity in LP and MP (Table S2). Consequently, our results demonstrated that
265 communities in LP and MP prevail by reducing LA to avoid damage at the expense of light capture.

Variability in g_s along an aridity gradient in TP was controlled by specific leaf area (SLA) (Table 1). Although a
significantly negative relationship was found between solar radiation and LA in this transect (Table S2), this negative effect
did not transfer to g_s (Table 1). We attributed this phenomenon to co-limitation of g_s by radiation and temperature. Plants
increase their leaf thickness to adapt to increasing temperature (Leigh *et al.*, 2012), and thick leaves have high heat capacity
270 to avoid damage from high temperature (Leigh *et al.*, 2012). SLA integrates leaf area and thickness, and generally decreases



with increasing radiation and drought stress, and increases with decreases in temperature (Poorter *et al.*, 2009). In this study, variability in SLA along an aridity gradient was significantly negatively correlated with maximum temperatures (Table S2). However, the direct effect of SLA on g_s in the structural equation was weak (Fig.4f). This effect may be obscured by drought stress.

275 5 Conclusions

This study highlighted the need to integrate multiple stressors and plant properties when determining spatial variability in stomatal conductance (g_s), and directly link species-level observations of physiological process (g_s) to ecosystem-level observations of functions at a large spatial scale. Specifically, our results demonstrated that excess radiation and low temperature interacted to exacerbate drought stress impacts on g_s among transects. Within a transect, radiation also exacerbated drought stress impacts on g_s . Effects of drought stress on g_s can be mitigated by decreasing temperatures in warm environments, and aggravated by increasing temperatures in cold environments. The primary determinant of drought stress on g_s was soil moisture in LP and MP, and vapor pressure deficit (VPD) in TP. The ability to predict variability in g_s could be significantly improved by integrating multiple stressors and leaf area in LP and TP, but not in TP due to an overwhelming effect of climate.

Data availability

285 Data availability. Requests for data or other materials should be directed to Xuefa Wen (wenxf@igsrr.ac.cn).

Author contributions

JW and XFW planned and designed the research. JW performed experiments and analyzed data. All authors jointly wrote the manuscript. All authors contributed critically to the drafts and gave final approval for publication.

Competing interests

290 The authors declare that they have no conflict of interest.

Acknowledgements

We thank the “Functional Trait database of terrestrial ecosystems in China (China_Traits)” for sharing all auxiliary plant and soil data. Ancillary meteorological data are available from China Meteorological Data Service Center (<http://data.cma.cn/>). This work was supported by the National Natural Science Foundation of China (41991234, 32001137).



295 References

- Aasamaa K., Sober A.: Responses of stomatal conductance to simultaneous changes in two environmental factors. *Tree Physiol.*, 31, 855-864, 2011. doi:10.1093/treephys/tpr078
- Aguirre-Gutierrez J., Oliveras I., Rifai S., Fauset S., Adu-Bredu S., Affum-Baffoe K., Baker T.R., Feldpausch T.R., Gvozdevaite A., Hubau W., Kraft N.J.B., Lewis S.L., Moore S., Niinemets U., Peprah T., Phillips O.L., Zieminska K., Enquist B., Malhi Y.: Drier tropical forests are susceptible to functional changes in response to a long-term drought. *Ecol. Lett.*, 22, 855-865, 2019. doi:10.1111/ele.13243
- Ainsworth E.A., Rogers A.: The response of photosynthesis and stomatal conductance to rising CO₂: mechanisms and environmental interactions. *Plant Cell Environ.*, 30, 258-270, 2007. doi:10.1111/j.1365-3040.2007.01641.x
- Anderegg W.R.L., Konings A.G., Trugman A.T., Yu K., Bowling D.R., Gabbitas R., Karp D.S., Pacala S., Sperry J.S., Sulman B.N., Zenes N.: Hydraulic diversity of forests regulates ecosystem resilience during drought. *Nature*, 561, 538-541, 2018. doi:10.1038/s41586-018-0539-7
- Barbour M.: Stable oxygen isotope composition of plant tissue: a review. *Functional Plant Biology*, 34, 83-94, 2007. doi:10.1071/fp06228
- Bowen G.J., Wassenaar L.I., Hobson K.A.: Global application of stable hydrogen and oxygen isotopes to wildlife forensics. *Oecologia*, 143, 337-348, 2005. doi:10.1007/s00442-004-1813-y
- Buckley T.N.: Modeling Stomatal Conductance. *Plant Physiology*, 174, 572-582, 2017. doi:10.1104/pp.16.01772
- Buckley T.N.: How do stomata respond to water status? *New Phytol.*, 224, 21-36, 2019. doi:10.1111/nph.15899
- Carminati A., Javaux M.: Soil Rather Than Xylem Vulnerability Controls Stomatal Response to Drought. *Trends Plant Sci*, 25, 868-880, 2020. doi:10.1016/j.tplants.2020.04.003
- Ciais P., Reichstein M., Viovy N., Granier A., Ogee J., Allard V., Aubinet M., Buchmann N., Bernhofer C., Carrara A., Chevallier F., De Noblet N., Friend A.D., Friedlingstein P., Grunwald T., Heinesch B., Keronen P., Knohl A., Krinner G., Loustau D., Manca G., Matteucci G., Miglietta F., Ourcival J.M., Papale D., Pilegaard K., Rambal S., Seufert G., Soussana J.F., Sanz M.J., Schulze E.D., Vesala T., Valentini R.: Europe-wide reduction in primary productivity caused by the heat and drought in 2003. *Nature*, 437, 529-533, 2005. doi:10.1038/nature03972
- Costa A.C., Rezende-Silva S.L., Megguer C.A., Moura L.M.F., Rosa M., Silva A.A.: The effect of irradiance and water restriction on photosynthesis in young jatoba-do-cerrado (*Hymenaea stigonocarpa*) plants. *Photosynthetica*, 53, 118-127, 2015. doi:10.1007/s11099-015-0085-6
- Cui X.Y., Tang Y.H., Gu S., Nishimura S., Shi S.B., Zhao X.Q.: Photosynthetic depression in relation to plant architecture in two alpine herbaceous species. *Environ. Exp. Bot.*, 50, 125-135, 2003. doi:10.1016/s0098-8472(03)00018-2
- Damour G., Simonneau T., Cochard H., Urban L.: An overview of models of stomatal conductance at the leaf level. *Plant Cell Environ.*, 33, 1419-1438, 2010. doi:10.1111/j.1365-3040.2010.02181.x
- Demmigadams B., Adams W.W.: Photoprotection and other responses of plants to high light stress. *Annu. Rev. Plant Physiol.*



- Plant Molec. Biol., 43, 599-626, 1992. doi:10.1146/annurev.pp.43.060192.003123
- 330 Deng J., Yao J., Zheng X., Gao G.: Transpiration and canopy stomatal conductance dynamics of Mongolian pine plantations in semi-arid deserts, Northern China. *Agricultural Water Management*, 249, 2021. doi:10.1016/j.agwat.2021.106806
- Doupis G., Chartzoulakis K.S., Taskos D., Patakas A.: The effects of drought and supplemental UV-B radiation on physiological and biochemical traits of the grapevine cultivar "Soultanina". *Oeno One*, 54, 2020. doi:10.20870/oeno-one.2020.54.4.3581
- 335 Duan B.L., Xuan Z.Y., Zhang X.L., Korpelainen H., Li C.Y.: Interactions between drought, ABA application and supplemental UV-B in *Populus yunnanensis*. *Physiologia Plantarum*, 134, 257-269, 2008. doi:10.1111/j.1399-3054.2008.01128.x
- Farquhar G.D., Caemmerer S.V., Berry J.A.: A biochemical-model of photosynthetic CO₂ assimilation in leaves of C3 species. *Planta*, 149, 78-90, 1980. doi:10.1007/bf00386231
- Flanagan L.B., Farquhar G.D.: Variation in the carbon and oxygen isotope composition of plant biomass and its relationship to water-use efficiency at the leaf- and ecosystem-scales in a northern Great Plains grassland. *Plant Cell Environ.*, 37, 425-340 438, 2014. doi:10.1111/pce.12165
- Flo V., Martinez-Vilalta J., Mencuccini M., Granda V., Anderegg W.R.L., Poyatos R.: Climate and functional traits jointly mediate tree water-use strategies. *New Phytol.*, 231, 617-630, 2021. doi:10.1111/nph.17404
- Fu Y.L., Yu G.R., Sun X.M., Li Y.N., Wen X.F., Zhang L.M., Li Z.Q., Zhao L., Hao Y.B.: Depression of net ecosystem CO₂ exchange in semi-arid *Leymus chinensis* steppe and alpine shrub. *Agric. For. Meteorol.*, 137, 234-244, 2006. 345 doi:10.1016/j.agrformet.2006.02.009
- Fyllas N.M., Bentley L.P., Shenkin A., Asner G.P., Atkin O.K., Diaz S., Enquist B.J., Farfan-Rios W., Gloor E., Guerrieri R., Huasco W.H., Ishida Y., Martin R.E., Meir P., Phillips O., Salinas N., Silman M., Weerasinghe L.K., Zaragoza-Castells J., Malhi Y.: Solar radiation and functional traits explain the decline of forest primary productivity along a tropical elevation gradient. *Ecol Lett*, 20, 730-740, 2017. doi:10.1111/ele.12771
- 350 Galmes J., Medrano H., Flexas J.: Photosynthetic limitations in response to water stress and recovery in Mediterranean plants with different growth forms. *New Phytol.*, 175, 81-93, 2007. doi:10.1111/j.1469-8137.2007.02087.x
- Grossiord C., Buckley T.N., Cernusak L.A., Novick K.A., Poulter B., Siegwolf R.T.W., Sperry J.S., McDowell N.G.: Plant responses to rising vapor pressure deficit. *New Phytol.*, 226, 1550-1566, 2020. doi:10.1111/nph.16485
- 355 Guerrieri R., Belmecheri S., Ollinger S.V., Asbjornsen H., Jennings K., Xiao J.F., Stocker B.D., Martin M., Hollinger D.Y., Bracho-Garrillo R., Clark K., Dore S., Kolb T., Munger J.W., Novick K., Richardson A.D.: Disentangling the role of photosynthesis and stomatal conductance on rising forest water-use efficiency. *Proceedings of the National Academy of Sciences of the United States of America*, 116, 16909-16914, 2019. doi:10.1073/pnas.1905912116
- Hoshika Y., Osada Y., de Marco A., Penuelas J., Paoletti E.: Global diurnal and nocturnal parameters of stomatal conductance in woody plants and major crops. *Glob. Ecol. Biogeogr.*, 27, 257-275, 2018. doi:10.1111/geb.12681
- 360 Jarvis P.G., McNaughton K.G.: Stomatal control of transpiration - scaling up from leaf to region. *Advances in Ecological Research*, 15, 1-49, 1986. doi:10.1016/s0065-2504(08)60119-1



- Kang X.M., Li Y.A., Zhou J.Y., Zhang S.T., Li C.X., Wang J.H., Liu W., Qi W.: Response of Leaf Traits of Eastern Qinghai-Tibetan Broad-Leaved Woody Plants to Climatic Factors. *Front. Plant Sci.*, 12, 2021. doi:10.3389/fpls.2021.679726
- 365 Konings A.G., Williams A.P., Gentine P.: Sensitivity of grassland productivity to aridity controlled by stomatal and xylem regulation. *Nat. Geosci.*, 10, 284-288, 2017. doi:10.1038/ngeo2903
- Lawrence M.G.: The relationship between relative humidity and the dewpoint temperature in moist air - A simple conversion and applications. *Bulletin of the American Meteorological Society*, 86, 225+, 2005. doi:10.1175/bams-86-2-225
- Leigh A., Sevanto S., Ball M.C., Close J.D., Ellsworth D.S., Knight C.A., Nicotra A.B., Vogel S.: Do thick leaves avoid thermal damage in critically low wind speeds? *New Phytol.*, 194, 477-487, 2012. doi:10.1111/j.1469-8137.2012.04058.x
- 370 Leuning R.: A critical-appraisal of a combined stomatal-photosynthesis model for C-3 plants. *Plant Cell Environ.*, 18, 339-355, 1995. doi:10.1111/j.1365-3040.1995.tb00370.x
- Li Z., Huang Y., Pan Y., Chen H., Hu G., Yang C.: Simulating response of the stomatal conductance of *Kobresia pygmaea* to environmental factors. *Acta Ecologica Sinica*, 40, 9094-9107, 2020.
- Liu H., Hu B., Wang Y., Liu G., Tang L., Ji D., Bai Y., Bao W., Chen X., Chen Y., Ding W., Han X., He F., Huang H., Huang
375 Z., Li X., Li Y., Liu W., Lin L., Ouyang Z., Qin B., Shen W., Shen Y., Su H., Song C., Sun B., Sun S., Wang A., Wang G., Wang H., Wang S., Wang Y., Wei W., Xie P., Xie Z., Yan X., Zeng F., Zhang F., Zhang Y., Zhang Y., Zhao C., Zhao W., Zhao X., Zhou G., Zhu B.: Two ultraviolet radiation datasets that cover China. *Adv. Atmos. Sci.*, 34, 805-815, 2017. doi:10.1007/s00376-017-6293-1
- Liu L.B., Gudmundsson L., Hauser M., Qin D.H., Li S.C., Seneviratne S.I.: Soil moisture dominates dryness stress on
380 ecosystem production globally. *Nat. Commun.*, 11, 9, 2020. doi:10.1038/s41467-020-18631-1
- Lyu S.D., Wang J., Song X.W., Wen X.F.: The relationship of delta D and delta O-18 in surface soil water and its implications for soil evaporation along grass transects of Tibet, Loess, and Inner Mongolia Plateau. *J. Hydrol.*, 600, 2021. doi:10.1016/j.jhydrol.2021.126533
- Martin-StPaul N., Delzon S., Cochard H.: Plant resistance to drought depends on timely stomatal closure. *Ecol. Lett.*, 20,
385 1437-1447, 2017.
- Medlyn B.E., Duursma R.A., Eamus D., Ellsworth D.S., Colin Prentice I., Barton C.V.M., Crous K.Y., de Angelis P., Freeman M., Wingate L.: Reconciling the optimal and empirical approaches to modelling stomatal conductance. *Glob. Change Biol.*, 18, 3476-3476, 2012. doi:10.1111/j.1365-2486.2012.02790.x
- Mercado L.M., Bellouin N., Sitch S., Boucher O., Huntingford C., Wild M., Cox P.M.: Impact of changes in diffuse radiation
390 on the global land carbon sink. *Nature*, 458, 1014-U1087, 2009. doi:10.1038/nature07949
- Moreno-Gutierrez C., Dawson T.E., Nicolas E., Querejeta J.I.: Isotopes reveal contrasting water use strategies among coexisting plant species in a Mediterranean ecosystem. *New Phytol.*, 196, 489-496, 2012. doi:10.1111/j.1469-8137.2012.04276.x
- Niu Z.G., He H.L., Zhu G.F., Ren X.L., Zhang L., Zhang K.: A spatial-temporal continuous dataset of the transpiration to evapotranspiration ratio in China from 1981-2015. *Sci. Data*, 7, 2020. doi:10.1038/s41597-020-00693-x
- 395 Oren R., Sperry J.S., Katul G.G., Pataki D.E., Ewers B.E., Phillips N., Schafer K.V.R.: Survey and synthesis of intra- and



- interspecific variation in stomatal sensitivity to vapour pressure deficit. *Plant Cell Environ.*, 22, 1515-1526, 1999. doi:10.1046/j.1365-3040.1999.00513.x
- Peguero-Pina J.J., Vilagrosa A., Alonso-Forn D., Ferrio J.P., Sancho-Knapik D., Gil-Pelegrin E.: Living in Drylands: Functional Adaptations of Trees and Shrubs to Cope with High Temperatures and Water Scarcity. *Forests*, 11, 2020. doi:10.3390/f11101028
- 400
- Peppe D.J., Royer D.L., Cariglino B., Oliver S.Y., Newman S., Leight E., Enikolopov G., Fernandez-Burgos M., Herrera F., Adams J.M., Correa E., Currano E.D., Erickson J.M., Hinojosa L.F., Hoganson J.W., Iglesias A., Jaramillo C.A., Johnson K.R., Jordan G.J., Kraft N.J.B., Lovelock E.C., Lusk C.H., Niinemets U., Penuelas J., Rapson G., Wing S.L., Wright I.J.: Sensitivity of leaf size and shape to climate: global patterns and paleoclimatic applications. *New Phytol.*, 190, 724-739, 2011. doi:10.1111/j.1469-8137.2010.03615.x
- 405
- Peters W., van der Velde I.R., van Schaik E., Miller J.B., Ciais P., Duarte H.F., van der Laan-Luijckx I.T., van der Molen M.K., Scholze M., Schaefer K., Vidale P.L., Verhoef A., Warlind D., Zhu D., Tans P.P., Vaughn B., White J.W.C.: Increased water-use efficiency and reduced CO₂ uptake by plants during droughts at a continental scale. *Nat. Geosci.*, 11, 744-+, 2018. doi:10.1038/s41561-018-0212-7
- 410
- Poorter H., Niinemets U., Poorter L., Wright I.J., Villar R.: Causes and consequences of variation in leaf mass per area (LMA): a meta-analysis. *New Phytol.*, 182, 565-588, 2009. doi:10.1111/j.1469-8137.2009.02830.x
- Schneider C.A., Rasband W.S., Eliceiri K.W.: NIH Image to ImageJ: 25 years of image analysis. *Nature Methods*, 9, 671-675, 2012. doi:10.1038/nmeth.2089
- Seneviratne S.I., Corti T., Davin E.L., Hirschi M., Jaeger E.B., Lehner I., Orlowsky B., Teuling A.J.: Investigating soil moisture–climate interactions in a changing climate: A review. *Earth-Sci. Rev.*, 99, 125–161, 2010.
- 415
- Stocker B.D., Zscheischler J., Keenan T.F., Prentice I.C., Seneviratne S.I., Penuelas J.: Drought impacts on terrestrial primary production underestimated by satellite monitoring. *Nat. Geosci.*, 12, 264-+, 2019. doi:10.1038/s41561-019-0318-6
- Wang H.B., Li X., Xiao J.F., Ma M.G.: Evapotranspiration components and water use efficiency from desert to alpine ecosystems in drylands. *Agric. For. Meteorol.*, 298, 2021. doi:10.1016/j.agrformet.2020.108283
- 420
- Wang J., Wen X.F., Lyu S., Guo Q.J.: Soil properties mediate ecosystem intrinsic water use efficiency and stomatal conductance via taxonomic diversity and leaf economic spectrum. *Sci. Total Environ.*, 783, 2021. doi:10.1016/j.scitotenv.2021.146968
- Wang Z., Wang C., Poulter B.: Responses of tree leaf gas exchange to elevated CO₂ combined with changes in temperature and water availability: A global synthesis. *Glob. Ecol. Biogeogr.*, 30, 2500-2512, 2021. doi:10.1111/geb.13394
- 425
- Wehr R., Commann R., Munger J.W., McManus J.B., Nelson D.D., Zahniser M.S., Saleska S.R., Wofsy S.C.: Dynamics of canopy stomatal conductance, transpiration, and evaporation in a temperate deciduous forest, validated by carbonyl sulfide uptake. *Biogeosciences*, 14, 389-401, 2017. doi:10.5194/bg-14-389-2017
- Wehr R., Saleska S.R.: Calculating canopy stomatal conductance from eddy covariance measurements, in light of the energy budget closure problem. *Biogeosciences*, 18, 13-24, 2021. doi:10.5194/bg-18-13-2021
- Wright I., Reich P., Westoby M., Ackerly D., Baruch Z., Bongers F., Cavender-Bares J., Chapin T., Cornelissen J.H.C., Diemer



- 430 M., Flexas J., Garnier E., Groom P.K., Gulias J., Hikosaka K., Lamont B.B., Lee T., Lee W., Lusk C., Midgley J.J., Navas
M.L., Niinemets U., Oleksyn J., Osada N., Poorter H., Poot P., Prior L., Pyankov V.I., Roumet C., Thomas S.C., Tjoelker
M.G., Veneklaas E.J., Villar R.: The worldwide leaf economics spectrum. *Nature*, 428, 821-827, 2004.
doi:10.1038/nature02403
- Wright I.J., Dong N., Maire V., Prentice I.C., Westoby M., Diaz S., Gallagher R.V., Jacobs B.F., Kooyman R., Law E.A.,
435 Leishman M.R., Niinemets U., Reich P.B., Sack L., Villar R., Wang H., Wilf P.: Global climatic drivers of leaf size. *Science*,
357, 917-921, 2017. doi:10.1126/science.aal4760
- Wright I.J., Leishman M.R., Read C., Westoby M.: Gradients of light availability and leaf traits with leaf age and canopy
position in 28 Australian shrubs and trees. *Functional Plant Biology*, 33, 407-419, 2006. doi:10.1071/fp05319
- Xia J.Y., Niu S.L., Ciais P., Janssens I.A., Chen J.Q., Ammann C., Arain A., Blanken P.D., Cescatti A., Bonal D., Buchmann
440 N., Curtis P.S., Chen S.P., Dong J.W., Flanagan L.B., Frankenberg C., Georgiadis T., Gough C.M., Hui D.F., Kiely G., Li
J.W., Lund M., Magliulo V., Marcolla B., Merbold L., Montagnani L., Moors E.J., Olesen J.E., Piao S.L., Raschi A.,
Roupsard O., Suyker A.E., Urbaniak M., Vaccari F.P., Varlagin A., Vesala T., Wilkinson M., Weng E., Wohlfahrt G., Yan
L.M., Luo Y.Q.: Joint control of terrestrial gross primary productivity by plant phenology and physiology. *Proceedings of
the National Academy of Sciences of the United States of America*, 112, 2788-2793, 2015. doi:10.1073/pnas.1413090112
- 445 Xu J.M., Wu B.F., Ryu D., Yan N.N., Zhu W.W., Ma Z.H.: A canopy conductance model with temporal physiological and
environmental factors. *Sci. Total Environ.*, 791, 2021. doi:10.1016/j.scitotenv.2021.148283
- Xu M.J., Zhang T., Zhang Y.J., Chen N., Zhu J.T., He Y.T., Zhao T.T., Yu G.R.: Drought limits alpine meadow productivity in
northern Tibet. *Agric. For. Meteorol.*, 303, 2021. doi:10.1016/j.agrformet.2021.108371
- Yao J.Y., Liu H.P., Huang J.P., Gao Z.M., Wang G.Y., Li D., Yu H.P., Chen X.Y.: Accelerated dryland expansion regulates future
450 variability in dryland gross primary production. *Nat. Commun.*, 11, 10, 2020. doi:10.1038/s41467-020-15515-2
- Yuan W.P., Zheng Y., Piao S.L., Ciais P., Lombardozzi D., Wang Y.P., Ryu Y., Chen G.X., Dong W.J., Hu Z.M., Jain A.K.,
Jiang C.Y., Kato E., Li S.H., Lienert S., Liu S.G., Nabel J., Qin Z.C., Quine T., Sitch S., Smith W.K., Wang F., Wu C.Y.,
Xiao Z.Q., Yang S.: Increased atmospheric vapor pressure deficit reduces global vegetation growth. *Sci. Adv.*, 5, 2019.
doi:10.1126/sciadv.aax1396
- 455 Zeuthen J., Mikkelsen T.N., PaludanMuller G., RoPoulsen H.: Effects of increased UV-B radiation and elevated levels of
tropospheric ozone on physiological processes in European beech (*Fagus sylvatica*). *Physiologia Plantarum*, 100, 281-
290, 1997. doi:10.1034/j.1399-3054.1997.1000209.x
- Zhang J.W., Guan K.Y., Peng B., Pan M., Zhou W., Jiang C.Y., Kimm H., Franz T.E., Grant R.F., Yang Y., Rudnick D.R.,
Heeren D.M., Suyker A.E., Bauerle W.L., Miner G.L.: Sustainable irrigation based on co-regulation of soil water supply
460 and atmospheric evaporative demand. *Nat. Commun.*, 12, 2021. doi:10.1038/s41467-021-25254-7
- Zhang T., Shen S., Cheng C.X.: Impact of radiations on the long-range correlation of soil moisture: A case study of the A'rou
superstation in the Heihe River Basin. *Journal of Geographical Sciences*, 29, 1491-1506, 2019. doi:10.1007/s11442-019-
1673-3



- 465 Zhang T., Zhang Y.J., Xu M.J., Zhu J.T., Chen N., Jiang Y.B., Huang K., Zu J.X., Liu Y.J., Yu G.R.: Water availability is more important than temperature in driving the carbon fluxes of an alpine meadow on the Tibetan Plateau. *Agric. For. Meteorol.*, 256, 22-31, 2018. doi:10.1016/j.agrformet.2018.02.027
- Zhang Z.Z., Zhao P., McCarthy H.R., Zhao X.H., Niu J.F., Zhu L.W., Ni G.Y., Ouyang L., Huang Y.Q.: Influence of the decoupling degree on the estimation of canopy stomatal conductance for two broadleaf tree species. *Agric. For. Meteorol.*, 221, 230-241, 2016. doi:10.1016/j.agrformet.2016.02.018
- 470 Zhu X.J., Yu G.R., Hu Z.M., Wang Q.F., He H.L., Yan J.H., Wang H.M., Zhang J.H.: Spatiotemporal variations of T/ET (the ratio of transpiration to evapotranspiration) in three forests of Eastern China. *Ecol. Indic.*, 52, 411-421, 2015. doi:10.1016/j.ecolind.2014.12.030